
Experimental identification of the position-dependent dynamics of an industrial manipulator

Monica K. Gonzalez¹, Bernd Peukert¹, Nikolas A. Theissen¹, Andreas Archenti^{1,2}

¹KTH Royal Institute of Technology, Department of Production Engineering, Manufacturing and Metrology Systems Division, 11428 Stockholm

²KTH Royal Institute of Technology, Department of Sustainable Production Development, 151 81 Södertälje

mgon@kth.se

Abstract

Industrial manipulators are desired to be commonly used for material removal applications due to their high flexibility, low cost, and large working space. However, their lower stiffness (compared to a machine tool) leads to a reduction in path accuracy. This reduction directly affects the dimensional accuracy of the machined part. Additionally, the low stiffness in the presence of dynamic process forces creates vibrations influencing the surface quality, tool life, and service life of the manipulator.

Static stiffness models, optimization, and compensation techniques exist to minimize force-induced deflections. Multi-body dynamics analytical models still lack the required accuracy in predicting the position-dependent dynamics of the manipulator. Dynamics data-driven models are rising to tackle the uncertainties in modeling the robot properties.

This study presents the position-dependent variation of the dynamic characteristics, namely frequency and damping, of a mid-size articulated industrial manipulator, which were determined through experimental modal analysis. The position-dependent dynamics is investigated and quantified in a low-frequency range and is discretely measured and presented in two perpendicular planes (horizontal and vertical) of the robot working space. The study concludes with a discussion on the potential to apply the dynamic information obtained experimentally for the process planning and working space optimization in contact applications.

Keywords: Industrial robot, dynamics, position-dependent, experimental modal analysis

1. Introduction

Industrial manipulators have been commonly used in the automation of manufacturing tasks such as pick-and-place, handling, assembling, welding, and painting. They have also been involved in machining tasks that require low cutting forces and lax Geometric Dimensions and Tolerances (GD&T), namely, trimming, deburring, polishing [1]. Among several aspects that stimulate the use of robots in other high-force operations, e.g., milling or drilling, their cost-effectiveness (lower cost for the same working space) and flexibility can be the leading ones. Furthermore, robots are an important option in terms of mobility and ease of installation, especially when manufacturing large-volume components or hard-to-reach areas on a complex part [2].

However, their main drawback is their higher compliance compared to machine tools, which results in lower accuracy in the presence of higher process forces [3]. In industrial manipulators, the accuracy of the machining operations does not solely rely on the preparation of the task programs, the robot path planning, and the motion strategy. It is also highly dependent on the robot behavior assessment inside the working space [1].

To address the issue of lower stiffness, research has been mainly focused on static stiffness modeling and joint stiffness identification [4]–[6]. These static stiffness models have been broadly used for pose optimization and deformation compensation, even for machining tasks which are characterized by time-varying loads [7]–[9]. The adoption of these models could be explained by their lower complexity entailing a reduced number of computation steps and effort for their implementation. Nevertheless, static models do not consider

the excitation of robot vibration modes due to the process forces and robot motion [10].

From the perspective of the dynamics, Pan and Zhang [11] indicated that mode coupling chatter (self-excited vibrations) was a dominant source of instability in robotic machining, where machining forces that act simultaneously in different directions tend to excite the lower frequency modes of the manipulator. Although multi-body modeling could be used to predict the robot's varying dynamic behavior in its working space, the majority of the existing models do not provide information on modal characteristics (frequency, damping, mode shape), which are of importance when predicting robotic machining stability [3].

Additionally, most of these models are a simplified version of the dynamics, do not account, e.g., for nonlinearities. In this regard, experimental results are more reliable since the real-time dynamic responses at the end-effector are obtained [12]. Nevertheless, the experimental identification of the Frequency Response Functions (FRFs) for all the postures is unfeasible. For this reason, research efforts focused on presenting dynamic characteristics in operational spaces, i.e., subsets of the working space in which the applications are to be conducted. Bisu et al. [13] analyzed the natural frequencies of an industrial manipulator at three discrete positions commonly used for machining composites and pointed out the influence of the robot positions on the natural frequencies' values. Mejri et al. [14] identified and quantified the tooltip dynamic properties' variations along machining trajectories, which consisted of ten points linearly distributed on the X-, Y- and Z-axis. In the aforementioned studies, significant variability in modal parameters was observed, which suggested that this effect needs to be taken into account in the process stability

prediction. Most recently, Karim et al. [15] and Bottin et al. [16] presented maps of the variation of the natural frequencies in first, second, and even third mode in vertical planes (the latter author in a so-called meridian which passes through the axis of joint 1). However, to the authors' knowledge, no previous study considered a volumetric section of the working space (intersection of two planes), and the previous variation analysis presented the natural frequencies, leaving aside the information on the modal damping, which has a direct influence in the machining stability.

This work aims to characterize the position-dependent dynamic behavior of the industrial manipulator in a section of the working space where a continuous machining process could be performed to indicate the influence of the variability of both natural frequency and damping in operational space.

2. Methodology

The scope of this analysis comprises an operational space represented by two planes, one vertical and one horizontal, that intersect each other, as shown in Figure 1. The planes are formed by 32 positions distributed along the two surfaces and can also be seen represented as robot targets in Figure 1. The corner positions of these two planes expressed in the Robot Base Coordinate system (RBCS) are included in Table 1.

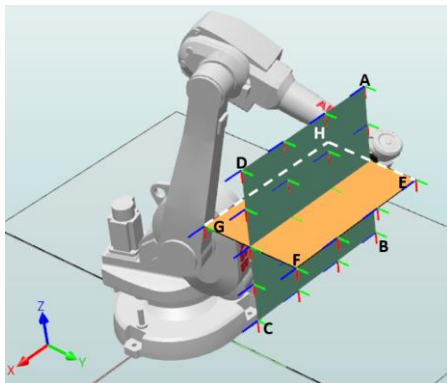


Figure 1. Location of the operational space of the study (vertical and horizontal planes) with respect to the RBCS.

Table 1. Corner positions of the horizontal and vertical planes expressed in the RBCS.

	Points	X Position/mm	Y Position /mm	Z Position /mm
Vertical	A	- 200	800	1 200
	B	- 200	800	600
	C	400	800	600
	D	400	800	1 200
Horizontal	E	- 200	1 000	900
	F	400	1 000	900
	G	400	600	900
	H	- 200	600	900

It is important to highlight that this section of the working space was selected taking into consideration kinematic singularities, so it is possible to guarantee a continuous linear movement in the planes with non-changing configurations, as is required, for instance, in conventional milling processes. Additionally, this section of the working space allows maintaining the same elbow-up solution in all the composing points, which reduces the influence of the changing moments of inertia in the analysis. Furthermore, only the robot structure was considered; no spindle or tool was mounted to disregard any influences of the end-effector coupling that could make the robot appear more compliant.

2.1. Measurement

An essential part of performing Experimental Modal Analysis (EMA) is to define the measurement concept. In this case, the applied concept was roving excitation, as it suffices for the extraction of damping and frequency characteristics, and the mode shapes were out of the scope of this work.

Ten different points on the robot structure were excited with an impact hammer, see Table 2. These excitation points were selected so that different excitation directions were applied. A soft Polyvinyl Chloride (PVC) hammer tip was to provide a longer excitation peak. This, in turn, results in a wider spectral excitation of the structure in the lower frequency range (below 100 Hz). The roving excitation concept has a lower risk of exciting structural nodes due to fixing points along the modal lines.

A triaxial accelerometer, see Table 2, was used to capture the response in the three Cartesian directions. The accelerometer was placed at the robot mechanical interface. Due to the Tool Center Point (TCP) orientation selection, the accelerometer was always aligned to the Cartesian directions of the RBCS. The information from all the directions was used in the modal parameter estimation process.

Each of the excitation points on the structure was excited 20 times, and the frequency response functions were obtained by averaging over all the impacts. This process was repeated for all the 32 points that constitute the vertical and horizontal plane. The force signal and the acceleration signal were recorded with a data acquisition system using two analog input modules, described in Table 2, with a sampling frequency of 5120 Hz.

Table 2. Measurement equipment utilized.

Equipment	Manufacturer	Model
Impact Hammer	Kistler	9726A5000
Triaxial Accelerometer	Dytran	3273A2
CompactDAQ Chassis	National Instruments	cDAQ-9189
Analogue Input modules (Sound and vibration)	National Instruments	NI-9234

2.2. Data Analysis

The time-domain signals were converted into the frequency domain, and the FRFs were obtained with the H1 estimator, which assumes no noise on the input signal. 960 FRFs (32 points x 3 response directions x 10 excitation points) were the input to a modal parameter Multiple Input Multiple Output (MIMO) implementation of the Algorithm of Mode Isolation (AMI)[17].

AMI begins with the generation of a composite FRF by averaging all FRFs. Then, it starts identifying the dominant peaks with a Single-Degree-of-Freedom (SDOF) Least-Squares-Complex-Frequency (LSCF) estimator and builds models in Rational Fraction Polynomial (RFP) form. Each identified mode is subtracted from the measurements until the desired number of dominant modes are fitted. Subsequently, the isolation stage starts. This stage iteratively isolates and refits each modal parameter until convergence criteria are met. Thus, the algorithm actually builds a true Multiple-Degree-of-Freedom (MDOF) model.

3. Results

The global modal properties, i.e., natural frequency and damping, were obtained for all 32 points. The position-dependent variation of the eigenfrequencies and the damping ratios for the first and second modes, which are the modes located in the lower frequency bandwidth, are presented in Figure 2.

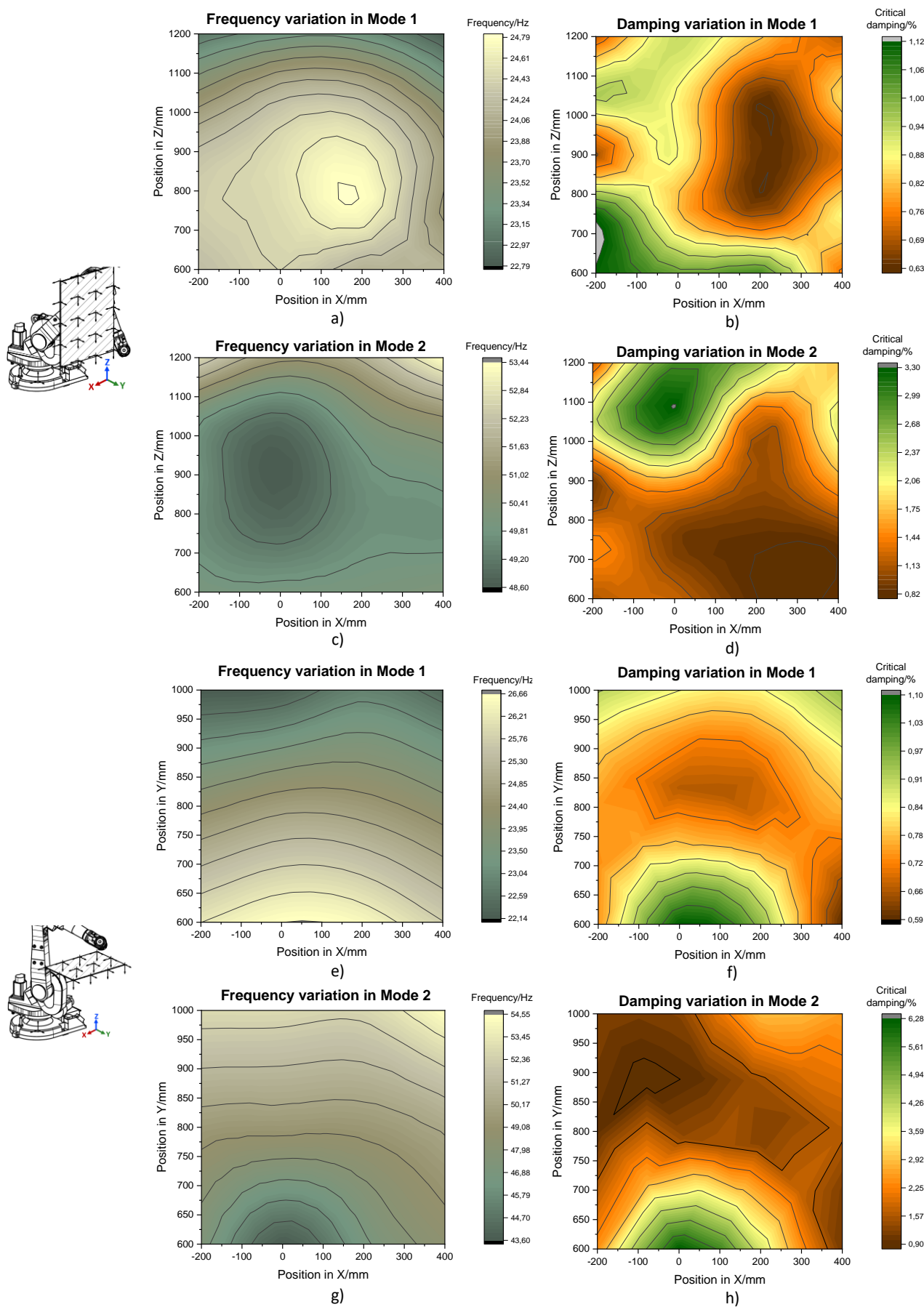


Figure 2. Eigenfrequency and damping ratio as a function of the position of the TCP: a) and b) the first mode in the vertical plane, c) and d) the second mode in the vertical plane, e) and f) the first mode in the horizontal plane, and g) and h) the second mode in the horizontal plane. In both planes, the position of the TCP represented in the pictures in the left-hand column corresponds to the lower-left corner (origin) of the contour plots.

Regarding the natural frequency, the vertical plane parameters vary approximately 8% (2Hz) for the first mode and around 9% (4.8Hz) for the second mode. These variations are higher in the horizontal plane, with approximately 17% (4.5Hz) for the first mode and 20% (11Hz) for the second one. This indicates that the variation of the eigenfrequencies might increase with the mode number. Therefore, in higher modes, higher frequency variation could be expected.

The widespread fact that fully stretched poses in manipulators present lower eigenfrequencies than retracted ones [15] can be seen in the first mode for vertical and horizontal planes, Figure 2 a) and e). However, the opposite behavior is shown in Figure 2 c) and g) for the second mode, where the eigenfrequency decreases in retracted positions. Thus, it could be stated that the assumption of the frequency dependence on the distance from the TCP to the centerline of Joint 1 only holds for the first mode, and different behaviors (or more complex ones) could be expected in higher-order modes. The frequency variation in the horizontal plane is seen as symmetric regarding the X-axis of the RBCS, which is expected.

When referring to the critical damping ratio, the analysis of the position-dependent variation increases in complexity. In general, an estimate for the damping will be less accurate than the one for the natural frequency [18]. The first mode is observed to be less damped than the second mode, and the percentage variation is on average 0.5%. The obtained values indicate that excitation of this mode should be highly avoided due to the low capability of the robot structure to dissipate this vibrational energy. As this behavior is seen in both planes, this consideration could be extended for the operational space under study. In the second mode, the variation of percentage of critical damping is higher and corresponds to roughly 3% in the vertical plane and 5% in the horizontal plane.

Another general remark from Figure 2 b), d), f), and h) is that there are different damping zones within the same working space that do not follow any particular distribution as in the eigenfrequencies' case. In the horizontal plane, more damped areas are located closer to the origin of the X-axis of the RBCS. However, as the TCP moves in the positive Y- direction, as shown in Figure 2 f) and h), the robot passes from a higher damping zone to a lower damping zone but then returns to a higher damping zone. In the vertical plane, for the first mode Figure 2 b), a higher damping zone corresponds to more retracted poses, and the movement of the TCP in the Z-axis positive direction will easily originate a jump to a lower damping zone. For the second mode Figure 2 d), most of the working space analyzed remains within a lower damping zone, and the damping starts to increase with the movement of the TCP in the positive Z-axis direction, which is contrary to the damping behavior observed for the first mode.

4. Conclusion

This work presents the variation of modal properties, i.e., eigenfrequencies and damping for an industrial manipulator as a function of the TCP position in a section of the working space. These properties are experimentally estimated in a low-frequency range (below 100 Hz), and the first two modes are analyzed. The properties' variation is shown and analyzed through intersecting vertical and horizontal planes in which manipulability is guaranteed to allow any high-force application.

The results highlight that even within a constricted operational space, the eigenfrequency and modal damping variation must be considered. In the eigenfrequency case, the variation could be as high as 10 Hz and increases with the mode order. The damping ratio difference is relatively low for the first mode (0.5%) but considerably high for the second mode (5%).

However, the first mode is less damped, and its excitation must be avoided.

Finally, the distribution of these parameters throughout the working space is critical when selecting an operational space that allows for a stable cutting process. When referring to machining operations, the knowledge of the robot's dynamic behavior is required to obtain higher workpiece quality with lower defects in the surface and geometric errors. Nevertheless, it is not possible to use an experimental procedure for each section of the working space. The next step will be to use these experimental data to build a data-driven dynamic behavior predictive model that could increase the comprehension of the robot dynamics to bigger sections of the working space.

Acknowledgements

The authors would like to thank VINNOVA, the Swedish innovation agency, and the SMART advanced manufacturing cluster for funding this research as a part of COMACH project (Grant Agreement ID: S0120). The authors would like to express their gratitude to the Center for Design and Management of Manufacturing Systems for their financial support.

References

- [1] A. Verl, A. Valente, S. Melkote, C. Brecher, E. Ozturk, and L. T. Tunc, "Robots in machining," vol. **68**, no. 2, pp. 799–822, 2019.
- [2] L. F. F. Furtado, E. Villani, L. G. Trabasso, and R. Sutério, "A method to improve the use of 6-dof robots as machine tools," *Int. J. Adv. Manuf. Technol.*, 2017.
- [3] H. N. Huynh, H. Assadi, E. Rivière-Lorphèvre, O. Verlinden, and K. Ahmadi, "Modelling the dynamics of industrial robots for milling operations," *Robot. Comput. Integr. Manuf.*, vol. **61**, 2020.
- [4] E. Abele, M. Weigold, and S. Rothenbücher, "Modeling and identification of an industrial robot for machining applications," *CIRP Ann. - Manuf. Technol.*, vol. **56**, no. 1, pp. 387–390, 2007.
- [5] C. Dumas *et al.*, "Joint Stiffness Identification of Industrial Serial Robots," *Robot. Comput. Integr. Manuf.*, **27** (4), pp.881-888, 2011
- [6] J. Zhou, H. N. Nguyen, and H. J. Kang, "Simultaneous identification of joint compliance and kinematic parameters of industrial robots," *Int. J. Precis. Eng. Manuf.*, 2014.
- [7] H. Xie, W. Li, and Z. Yin, "Posture Optimization Based on Both Joint Parameter Error and Stiffness for Robotic Milling", *Intelligent Robotics and Applications*, 2018, pp. 277–286.
- [8] A. Klimchik *et al.*, "Calibration of Industrial Robots with Pneumatic Gravity Compensators", *IEEE International Conference on Advanced Intelligent Mechatronics*, 2017.
- [9] G. Li, F. Zhang, Y. Fu, and S. Wang, "Joint stiffness identification and deformation compensation of serial robots based on dual quaternion algebra," *Appl. Sci.*, vol. **9**, no. 1, 2018.
- [10] T. Cvitanic, V. Nguyen, and S. N. Melkote, "Pose optimization in robotic machining using static and dynamic stiffness models," *Robot. Comput. Integr. Manuf.*, vol. **66**, p. 101992, 2020.
- [11] Z. Pan, H. Zhang, Z. Zhu, and J. Wang, "Chatter analysis of robotic machining process," *J. Mater. Process. Technol.*, 2006.
- [12] C. Chen *et al.*, "Stiffness performance index based posture and feed orientation optimization in robotic milling process," *Robot. Comput. Integr. Manuf.*, 2019.
- [13] C. Bisu, M. Cherif, A. Gerard, and J.-Y. K'nevez, "Dynamic behavior analysis for a six axis industrial machining robot," *Adv. Mater. Res.*, vol. **423**, pp. 65–76, 2012.
- [14] S. Mejri, V. Gagnol, T. P. Le, L. Sabourin, P. Ray, and P. Paultre, "Dynamic characterization of machining robot and stability analysis," *Int. J. Adv. Manuf. Technol.*, vol. **82**, pp. 351–359, 2016.
- [15] A. Karim, J. Hitzer, A. Lechler, and A. Verl, "Analysis of the dynamic behavior of a six-axis industrial robot within the entire workspace in respect of machining tasks," *IEEE/ASME Int. Conf. Adv. Intell. Mechatronics*, pp. 670–675, 2017.
- [16] M. Bottin, S. Cocuzza, N. Comand, and A. Doria, "Modeling and Identification of an Industrial Robot with a Selective Modal Approach," *Applied Sciences*, vol. **10**, no. 13, 2020.
- [17] M. S. Allen, "Global and Multi-Input-Multi-Output (MIMO) Extensions of the Algorithm of Mode Isolation (AMI)", 2005.
- [18] D. J. Ewins, "Modal Testing: Theory, Practice and Application," p. 562, 2009.